

Two-Color QCD with Chiral Chemical Potential ¹

V. V. Braguta*, V. A. Goy[†], E.-M. Ilgenfritz**, A. Yu. Kotov*, A. V. Molochkov[†],
M. Müller-Preussker[‡], B. Petersson[‡] and A. Schreiber[‡]

**Institute of Theoretical and Experimental Physics, 117218 Moscow, Russia*

[†]Far Eastern Federal University, School of Biomedicine, 690950 Vladivostok, Russia

***Joint Institute for Nuclear Research, VBLHEP and BLTP, 141980 Dubna, Russia*

[‡]Humboldt-Universität zu Berlin, Institut für Physik, 12489 Berlin, Germany

Abstract. The phase diagram of two-color QCD with a chiral chemical potential is studied on the lattice. The focus is on the confinement/deconfinement phase transition and the breaking/restoration of chiral symmetry. The simulations are carried out with dynamical staggered fermions without rooting. The dependence of the Polyakov loop, the chiral condensate and the corresponding susceptibilities on the chiral chemical potential and the temperature are presented.

Keywords: Lattice gauge theory, deconfinement, chiral symmetry breaking, phase transition, chiral density

PACS: 12.38.Aw, 12.38.Gc, 11.15.Ha

INTRODUCTION

For the vacuum state of QCD and the properties of low-temperature QCD the existence of non-trivial topological excitations is important. Well known are instantons [1] as classical solutions in Euclidean space. The role of topology for the solution of the famous $U_A(1)$ problem has been recognized very early [2, 3].

It is known by now from lattice QCD that the (fractal) dimensionality of the topological structures in the vacuum depends very strongly on the resolution scale [4]. In particular, infrared instantons structures are believed to explain chiral symmetry breaking [5, 6].

The gluon fields contributing to the path integral at finite temperature correspondingly may contain calorons [7, 8]. Because of non-trivial holonomy they consist of dyons and therefore, have a richer structure than instantons. Their changes they experience at the QCD phase transition are presently under study [9, 10].

Some time ago the gluonic topological structure and the famous axial anomaly have been proposed to be immediately observable (and controllable) through the generation of P and CP violating domains in heavy ion collisions [11, 12]. It has been demonstrated by detailed numerical calculations [11, 13] that macroscopic domains of (anti)parallel color-electric and color-magnetic field can emerge in a heavy ion collision creating an increasing chiral imbalance among the quarks which are deconfined due to the high temperature. In this situation, the magnetic field created by the spectator nucleons may initiate a charge separation relative to the reaction plane (parallel to the electro-magnetic field) [14]. The resulting charge asymmetry of quarks would become observable in terms of recombined hadrons (chiral-magnetic effect) [15, 16]. The strength (and particularly the dependence on the collision energy) of this effect has been theoretically studied and proposed to be a measure for the transient existence of liberated quarks [11, 12, 17].

In recent years the dependence of the chiral and deconfinement transitions on the magnetic field has been investigated both in models and ab-initio lattice simulations, see e.g. [18, 19]. It remains an open question whether the phase transition from quarks to hadrons, i.e. the onset of confinement and chiral symmetry breaking (and vice versa), depends on the chiral imbalance.

In this article we study the change of the phase structure by an equilibrium lattice simulation. We mimic the topological content (of a topologically nontrivial gluonic background in heavy ion collisions) by a standard of chiral imbalance, which is provided by a chiral chemical condensate. In this form, the modification of the phase diagram by the chiral chemical potential μ_5 has been studied mainly in effective models [20, 21, 22, 23, 24] with which we will

¹ This paper is based on talks given by A. Yu. Kotov at Conferences ‘LATTICE ’14’, New York, 2014 and ‘QCHS XI’, St. Petersburg, 2014.

compare our results.

On the lattice, contrary to the ordinary chemical potential (for quarks, i.e. baryonic charge), simulations with non-zero μ_5 are not hampered by a sign problem. They are accessible to standard hybrid Monte Carlo algorithms. Such lattice simulations with $\mu_5 \neq 0$ were already performed in Ref. [25, 26]. The main goal of these papers, however, was the chiral magnetic effect. Therefore, the phase diagram was not systematically studied.

In our study we perform simulations with the $SU(2)$ gauge group. One reason is that less computational resources are required for this pilot study than for full QCD. The second one is that we have already carried out two-colour QCD computations with an external magnetic field [27, 28].

DETAILS OF THE SIMULATIONS

We have performed simulations with the $SU(2)$ gauge group. We employ the standard Wilson plaquette action

$$S_g = \beta \sum_{x,\mu < \nu} \left(1 - \frac{1}{N_c} \text{Tr} U_{\mu\nu}(x) \right). \quad (1)$$

For the fermionic part of the action we use staggered fermions

$$S_f = ma \sum_x \bar{\psi}_x \psi_x + \frac{1}{2} \sum_{x\mu} \eta_\mu(x) (\bar{\psi}_{x+\hat{\mu}} U_\mu(x) \psi_x - \bar{\psi}_x U_\mu^\dagger(x) \psi_{x+\hat{\mu}}) + \frac{1}{2} \mu_5 a \sum_x s(x) (\bar{\psi}_{x+\hat{\delta}} \bar{U}_{x+\hat{\delta},x} \psi_x - \bar{\psi}_x \bar{U}_{x+\hat{\delta},x}^\dagger \psi_{x+\hat{\delta}}), \quad (2)$$

where the $\eta_\mu(x)$ are the standard staggered phase factors: $\eta_1(x) = 1$, $\eta_\mu(x) = (-1)^{x_1 + \dots + x_{\mu-1}}$ for $\mu = 2, 3, 4$. Furthermore, a denotes the lattice spacing, m the bare fermion mass, and μ_5 the value of the chiral chemical potential. In the chirality breaking term $s(x) = (-1)^{x_2}$, $\hat{\delta} = (1, 1, 1, 0)$ represents a shift to a diagonally located site of a spatial elementary cube. The combination $\bar{U}_{x+\hat{\delta},x} = \frac{1}{6} \sum_{i,j,k=\text{perm}(1,2,3)} U_i(x+\hat{e}_j+\hat{e}_k) U_j(x+\hat{e}_k) U_k(x)$ is connecting sites x and

$x + \hat{\delta}$ symmetrized over the 6 shortest paths between these sites. In the continuum limit Eq. (2) can be rewritten in the Dirac spinor-flavor basis [29, 30] as follows

$$S_f \rightarrow S_f^{(cont)} = \int d^4x \sum_{i=1}^4 \bar{q}_i (\partial_\mu \gamma_\mu + ig A_\mu \gamma_\mu + m + \mu_5 \gamma_5 \gamma_4) q_i. \quad (3)$$

It should be noted here that the usual baryonic chemical potential [31] and also the chiral chemical potential [26] are introduced to the action as a modification of the temporal links by corresponding exponential factors in order to eliminate chemical potential dependent quadratic divergencies. For staggered fermions this modification can be performed as well for the baryonic chemical potential. However, for the chiral chemical potential such a modification leads to a highly non-local action [26]. Therefore, we decided to introduce μ_5 in Eq. (2) in an additive way similar to the mass term leaving aside the question of arising singularities for the time being. We expect that the Polyakov loop will not contain μ_5 dependent singular terms.

We have performed simulations with two lattice sizes $N_\tau \times N_\sigma^3 = 6 \times 16^3, 10 \times 28^3$. The measured observables are

- the Polyakov loop

$$L = \frac{1}{N_\sigma^3} \sum_{n_1, n_2, n_3} \langle \text{Tr} \prod_{n_4=1}^{N_\tau} U_4(n_1, n_2, n_3, n_4) \rangle, \quad (4)$$

- the chiral condensate

$$a^3 \langle \bar{\psi} \psi \rangle = - \frac{1}{N_\tau N_\sigma^3} \frac{1}{4} \frac{\partial}{\partial (ma)} \log Z = \frac{1}{N_\tau N_\sigma^3} \frac{1}{4} \langle \text{Tr} \frac{1}{D + ma} \rangle, \quad (5)$$

- the Polyakov loop susceptibility

$$\chi_L = N_\sigma^3 (\langle L^2 \rangle - \langle L \rangle^2), \quad (6)$$

- the disconnected part of the chiral susceptibility

$$\chi_{disc} = \frac{1}{N_\tau N_\sigma^3} \frac{1}{16} (\langle (\text{Tr} \frac{1}{D+ma})^2 \rangle - \langle \text{Tr} \frac{1}{D+ma} \rangle^2). \quad (7)$$

The Polyakov loop and the corresponding susceptibility are sensitive to the confinement/deconfinement phase transition, while the chiral condensate in principle responds to chiral symmetry breaking/restoration.

The simulations have been carried out with a CUDA code to run the Hybrid Monte Carlo algorithm on GPU's. The dependence of the lattice spacing on the coupling parameter β was taken from [27]. For our simulations with the lattice size 6×16^3 the fermion mass was kept fixed in lattice units at $ma = 0.01$ while changing β . E.g. for $\beta = 1.80$ this corresponds to a pion mass value $m_\pi \approx 330$ MeV. For the larger lattice size 10×28^3 and for various β values we have chosen the same bare quark mass in physical units $m \simeq 19$ MeV, which corresponds to $m_\pi \approx 540$ MeV.

RESULTS AND CONCLUSIONS

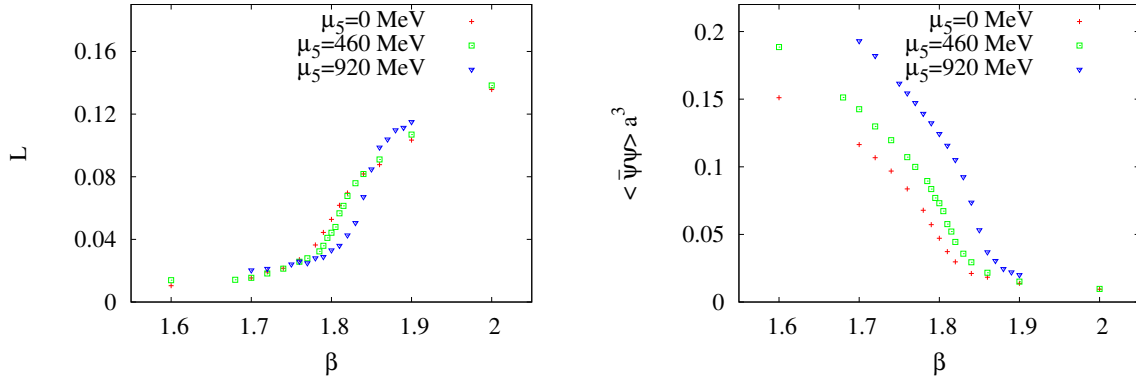


Figure 1. Polyakov loop (left) and chiral condensate (right) versus β for three μ_5 values and lattice size 6×16^3 . Errors are smaller than the data point symbols.

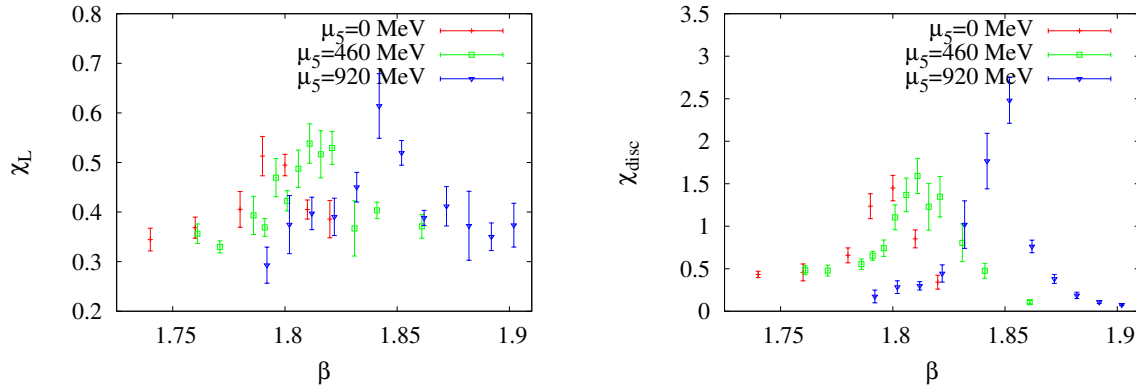


Figure 2. Polyakov loop susceptibility (left) and chiral susceptibility (right) versus β for three values of μ_5 and lattice size 6×16^3 . In order to avoid a complete superposition of data points belonging to different μ_5 values we applied a tiny shift along the β axis.

For the smaller lattice (6×16^3) we present results for three fixed values of $\mu_5 = 0, 460, 920$ MeV and for different values of β , while the bare fermion mass remained constant in lattice units $ma = 0.01$. The results for the Polyakov loop and the chiral condensate are plotted in Fig. 1. We see that increasing chiral chemical potential moves the position of the deconfinement and chiral transition, respectively, to larger values of β . This means that the transition temperature

increases. Plots for the chiral susceptibility and the Polyakov loop susceptibility (see Fig. 2) confirm this observation. We estimate the change of the critical temperature to be $\frac{T_c(\mu_5) - T_c(0)}{T_c(0)} \sim 20\%$ for $\mu_5 = 920$ MeV. The results do not show any splitting between the chiral and the deconfinement transition.

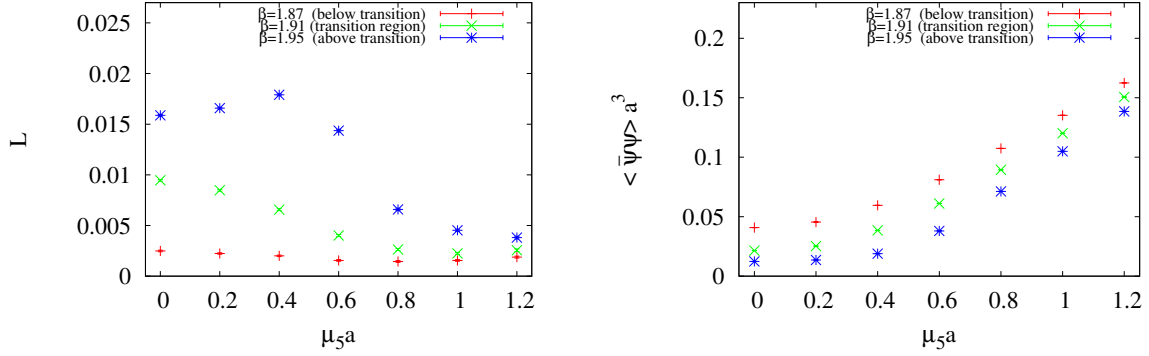


Figure 3. Polyakov loop (left) and chiral condensate (right) versus $\mu_5 a$ for three fixed values of β and lattice size 10×28^3 .

To confirm our results we carried out simulations also for the larger lattice size 10×28^3 . In Fig. 3 we present results for varying μ_5 and fixed values of $\beta = 1.87, 1.91$ and 1.95 , which for a vanishing chiral chemical potential correspond to temperatures below the transition, to the transition region, and to the high temperature phase, respectively. As can be seen from this figure, in the confinement phase the Polyakov loop remains almost constant with increasing chiral chemical potential. It means, that if the system was in the confinement phase at $\mu_5 = 0$, it remains confined at $\mu_5 > 0$. Moreover, we observe the Polyakov loop to drop down both in the deconfinement phase and in the transition region. Thus, the system goes into the confinement phase for sufficiently large μ_5 . With other words, we conclude that the critical temperature increases with an increasing chiral chemical potential in agreement with our results obtained on the smaller lattice. Notice that in case of the larger lattice we have kept fixed the bare fermion mass in physical units at $m \simeq 19$ MeV for all three β values, while changing μ_5 . It is worth mentioning that the behavior described above looks quite similar as that obtained for two-color QCD in an external magnetic field [27, 9].

Our results are in contradiction to those of the models studied in [20, 21, 22], where the critical temperature of the transition was observed to decrease. Furthermore, in these papers at some critical value of the chiral chemical potential the transition was reported to become first order. In our simulations we do not see such a behavior. However, the results obtained have a tendency towards a sharper phase transition at nonzero chiral chemical potential.

Although the analytic results are only derived in models and not in full QCD also in our approach there are some differences to QCD. We use the $SU(2)$ gauge group instead of $SU(3)$ and four flavor degrees of freedom. Moreover, the pion mass value used here is higher than the physical one. The situation can change, when one arrives at smaller quark masses. We want to address this question in a future work.

ACKNOWLEDGMENTS

The authors are grateful to V. I. Zakharov and V. G. Bornyakov for interesting and stimulating discussions. The simulations were performed at GPUs of supercomputer K100 and computers of the Berlin group. The work was supported by FEFU grants No. 12-02-13000-FEFU_a and 13-09-617-m_a, RFBR grants 14-02-01185-a, 13-02-01387-a, grant of the president of the RF MD-3215.2014.2 and grant of the FAIR-Russia Research Center.

REFERENCES

1. A. A. Belavin, A. M. Polyakov, A. S. Shvarts, and Y. S. Tyupkin, *Phys. Lett.* **B59**, 85 (1975).
2. E. Witten, *Nucl. Phys.* **B156**, 269 (1979).

3. G. Veneziano, *Nucl. Phys.* **B159**, 213 (1979).
4. E.-M. Ilgenfritz, D. Leinweber, P. Moran, K. Koller, G. Schierholz, and V. Weinberg, *Phys.Rev.* **D77**, 074502 (2008), 0801.1725.
5. T. Schäfer, and E. V. Shuryak, *Rev.Mod.Phys.* **70**, 323–426 (1998), hep-ph/9610451.
6. V. Shuryak, E. and T. Schäfer, *Nucl.Phys.Proc.Suppl.* **53**, 472–474 (1997).
7. T. C. Kraan, and P. van Baal, *Nucl.Phys.* **B533**, 627–659 (1998), hep-th/9805168.
8. K.-M. Lee, and C.-H. Lu, *Phys.Rev.* **D58**, 025011 (1998), hep-th/9802108.
9. E.-M. Ilgenfritz, B. Martemyanov, and M. Müller-Preussker, *Phys.Rev.* **D89**, 054503 (2014), 1309.7850.
10. V. G. Bornyakov, E.-M. Ilgenfritz, B. V. Martemyanov, and M. Müller-Preussker (2014), 1410.4632.
11. D. E. Kharzeev, *Phys.Lett.* **B633**, 260 (2006), hep-ph/0406125.
12. K. Fukushima, D. E. Kharzeev, and H. J. Warringa, *Phys.Rev.* **D78**, 074033 (2008), 0808.3382.
13. D. E. Kharzeev, A. Krasnitz, and R. Venugopalan, *Phys.Lett.* **B545**, 298–306 (2002), hep-ph/0109253.
14. D. E. Kharzeev, L. D. McLerran, and H. J. Warringa, *Nucl.Phys.* **A803**, 227 (2008), 0711.0950.
15. B. I. Abelev, et al., *Phys.Rev.Lett.* **103**, 251601 (2009), 0909.1739.
16. B. I. Abelev, et al., *Phys.Rev.* **C81**, 054908 (2010), 0909.1717.
17. L. Adamczyk, et al., *Phys.Rev.Lett.* **113**, 052302 (2014), 1404.1433.
18. I. A. Shovkovy, *Lect.Notes Phys.* **871**, 13 (2013), 1207.5081.
19. M. D’Elia, *Lect.Notes Phys.* **871**, 181 (2013), 1209.0374.
20. K. Fukushima, M. Ruggieri, and R. Gatto, *Phys.Rev.* **D81**, 114031 (2010), 1003.0047.
21. M. N. Chernodub, and A. S. Nedelin, *Phys.Rev.* **D83**, 105008 (2011), 1102.0188.
22. R. Gatto, and M. Ruggieri, *Phys.Rev.* **D85**, 054013 (2012), 1110.4904.
23. A. A. Andrianov, D. Espriu, and X. Planells, *Eur.Phys.J.* **C74**, 2776 (2014), 1310.4416.
24. X. Planells, A. A. Andrianov, V. A. Andrianov, and D. Espriu, *PoS QFTHEP2013*, 049 (2013), 1310.4434.
25. A. Yamamoto, *Phys.Rev.Lett.* **107**, 031601 (2011), 1105.0385.
26. A. Yamamoto, *Phys.Rev.* **D84**, 114504 (2011), 1111.4681.
27. E.-M. Ilgenfritz, M. Kalinowski, M. Müller-Preussker, B. Petersson, and A. Schreiber, *Phys.Rev.* **D85**, 114504 (2012), 1203.3360.
28. E.-M. Ilgenfritz, M. Müller-Preussker, B. Petersson, and A. Schreiber, *Phys.Rev.* **D89**, 054512 (2014), 1310.7876.
29. H. Kluberg-Stern, A. Morel, O. Napoly, and B. Petersson, *Nucl.Phys.* **B220**, 447 (1983).
30. I. Montvay, and G. Münster, *Quantum fields on a lattice*, Cambridge University Press, 1994.
31. P. Hasenfratz, and F. Karsch, *Phys.Lett.* **B125**, 308 (1983).